SPEKTRA: Jurnal Fisika dan Aplikasinya
Volume 10, Issue 1, April 2025
Homepage: doi.org/10.21009/SPEKTRA

DOI: doi.org/10.21009/SPEKTRA.101.04

Non-Relativistic Quantum Particle Confined on a Cylindrical Surface under a Stark-like Potential

Deriyan Senjaya*

Department of Physics, National Tsing Hua University, Hsinchu 30013, Taiwan

*Corresponding Author Email: d_senjaya@gapp.nthu.edu.tw

Received: 12 February 2025
Revised: 1 April 2025
Accepted: 15 April 2024
Online: 21 April 2025
Published: 30 April 2025

SPEKTRA: Jurnal Fisika dan Aplikasinya
p-ISSN: 2541-3384
e-ISSN: 2541-3392

ABSTRACT

This study explores the influence of a Stark-like perturbative potential on a quantum particle confined to a cylindrical surface (QPCS) and its implications for extra-dimensional theories. The QPCS framework is particularly relevant to Kaluza-Klein (KK) theory, which postulates extra spatial dimensions to unify electromagnetism and gravity. In KK theory, these extra dimensions are typically hidden and require high-energy conditions for detection. Motivated by the challenge of uncovering these dimensions more feasibly, this research applies a perturbative potential of the form $\widehat{H}_{SL} = \beta z V_{o_z}(\theta)$ to a QPCS characterized by length L and radius R_o. This potential is inspired by the Stark effect in hydrogen atoms, where energy level splitting serves as an indicator of an external influence. The study demonstrates that, for a degenerate configuration ($R_o = L/\pi$), the Stark-like perturbation effectively induces energy level splitting, which can be interpreted as a means of revealing hidden dimensions. The first-order energy correction in this scenario depends explicitly on the quantum numbers n_z and n_θ, highlighting the potential for this approach to probe extra-dimensional effects in lower-energy quantum systems.

Keywords: Kaluza-Klein theory, extra dimension, quantum particle, Stark-like potential, perturbation theory

INTRODUCTION

The combination of gravitational and electromagnetic interactions is well described by Kaluza-Klein (KK) theory, which introduces an extra spatial dimension x^5. This hidden extra dimension offers an explanation for why gravity appears weaker than electromagnetism [1, 2, 3]. However, detecting x^5 requires high-energy perturbations [3], making direct experimental

verification challenging, such as in the Large Hadron Collider (LHC). This difficulty raises fundamental questions about the existence of extra dimensions.

To explore this issue, this paper investigates the behavior of a Quantum Particle Confined on a Cylindrical Surface (QPCS) under a Stark-like perturbative potential. The QPCS serves as a simplified quantum system that mirrors key aspects of KK theory [4, 5]. Specifically, a compactified extra dimension can be visualized as a small, periodic direction perpendicular to ordinary space (the θ-direction), allowing higher-dimensional theories to manifest in lower-dimensional settings while preserving geometric properties [5]. The choice of a Stark-like potential is inspired by its role in splitting energy levels in the hydrogen atom [6, 7]. Similarly, applying this perturbative potential to the QPCS could induce an energy-splitting effect, providing insight into how an extra dimension might be revealed within a quantum system.

A QUANTUM PARTICLE CONFINED ON A CYLINDRICAL SURFACE (QPCS)

Consider a non-relativistic free particle of mass m confined on the surface of a cylinder with radius R_o and length L, as shown in FIGURE 1. In the quantum mechanics picture, the behavior of the particle in this system is well described by the Schrödinger equation in EQUATION (1), using the cylindrical coordinates (r, θ, z), with $\hat{V} = 0$ for $0 \leq z \leq L$ and $0 \leq \theta \leq 2\pi$.

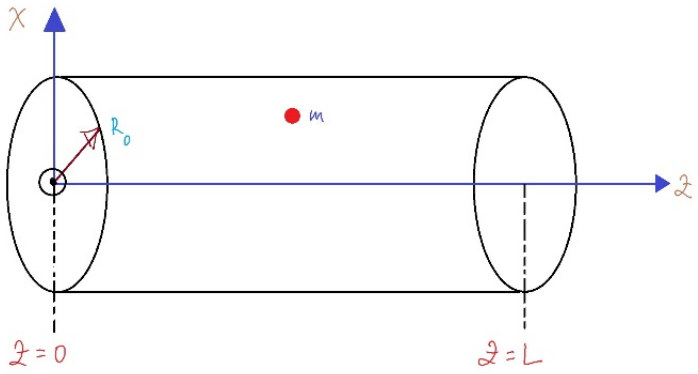

FIGURE 1. Quantum particles on the surface of a cylinder

$$-\frac{\hbar^2}{2m}\left[\frac{1}{r}\frac{\partial}{\partial r}\left(r\frac{\partial \Psi}{\partial r}\right)+\frac{1}{r^2}\frac{\partial^2 \Psi}{\partial \theta^2}+\frac{\partial^2 \Psi}{\partial z^2}\right]=E\Psi \tag{1}$$

Here, the $\Psi = \Psi(r, \theta, z, 0)$ indicates the particle's wave function at $t = 0$, and E is the particle's energy. To solve EQUATION (1), one can use the trial function (*ansatz*) of variable separation in the following form:

$$\Psi(r, \theta, z, 0) = R(r)\Theta(\theta)Z(z) \tag{2}$$

$R(r)$ is a function that only depends on r, $\Theta(\theta)$ is a function that only depends on the θ, and $Z(z)$ is a function that only depends on z. Substituting EQUATION (2) into the Schrödinger equation and dividing all sides by $R\Theta Z$ and $-\hbar^2/2m$, one can obtain:

$$\frac{1}{rR}\frac{d}{dr}\left(r\frac{dR}{dr}\right)+\frac{1}{r^2\Theta}\frac{d^2\Theta}{d\theta^2}+\frac{1}{Z}\frac{d^2Z}{dz^2}=-\frac{2mE}{\hbar^2} \quad (3)$$

For the free particle on the surface of a cylinder, there is a fact that helps reduce the complexity of EQUATION (3). The particle on the surface of a cylinder always has a constraint of motion at $r = R_o$. Therefore, the Ψ only depends on two variables, θ and z. Let $R(r)$ be a constant, then the differential form of dR/dr in EQUATION (3) will vanish, and EQUATION (3) turns out to be EQUATION (4) as follows:

$$\frac{1}{\Theta}\frac{d^2\Theta}{d\theta^2}+\frac{R_o^2}{Z}\frac{d^2Z}{dz^2}=-\frac{2mER_o^2}{\hbar^2} \quad (4)$$

Let the first and second terms of the left-hand side of EQUATION (4) be constants U^2 and V^2, respectively. Then, one can find two separable equations, as shown in EQUATION (5) and EQUATION (6) below.

$$\frac{1}{\Theta}\frac{d^2\Theta}{d\theta^2}=-U^2\rightarrow\frac{d^2\Theta}{d\theta^2}+U^2\Theta=0 \quad (5)$$

$$\frac{R_o^2}{Z}\frac{d^2Z}{dz^2}=-V^2\rightarrow\frac{d^2Z}{dz^2}+\frac{V^2Z}{R_o^2}=0 \quad (6)$$

EQUATION (5) and EQUATION (6) are two second-order ordinary differential equations (ODEs) with an oscillation-like model. Therefore, the general solutions for EQUATION (5) and EQUATION (6) are:

$$\Theta(\theta)=C_1e^{iU\theta}+C_2e^{-iU\theta} \quad (7)$$

$$Z(z)=C_3\sin\left(\frac{Vz}{R_o}\right)+C_4\cos\left(\frac{Vz}{R_o}\right) \quad (8)$$

Based on EQUATION (5) and EQUATION (6) general solutions, one can conclude the general solution of $\Psi(\theta,z,0)$ is expressed in EQUATION (9) below. The complete wave function of the system can be obtained using the appropriate boundary conditions.

$$\Psi(\theta,z,0)=\left[C_3\sin\left(\frac{Vz}{R_o}\right)+C_4\cos\left(\frac{Vz}{R_o}\right)\right]\left[C_1e^{iU\theta}+C_2e^{-iU\theta}\right] \quad (9)$$

First Boundary Condition

The particle in the θ-direction moves in a clockwise (CW) or counterclockwise (CCW) direction only. The particle in this direction cannot move back and forth. Therefore, mathematically speaking, one can safely assume that $C_2 = 0$. By this boundary condition, EQUATION (9) is reduced to EQUATION (10) as follows:

$$\Psi(\theta,z,0)=C_1\left[C_3\sin\left(\frac{Vz}{R_o}\right)+C_4\cos\left(\frac{Vz}{R_o}\right)\right]e^{iU\theta} \quad (10)$$

The particle in the θ-direction also moves periodically. So, one can find that the wave function EQUATION (10) should fulfill the periodic boundary condition $\Psi(0,z,0)=\Psi(2\pi,z,0)\rightarrow$

$e^{2\pi iU} = 1$. Using the periodic boundary condition, the solution of U should be n_θ. The n_θ is called the θ-Quantum number and takes integer values ($n_\theta = 1, 2, 3, ...$). Therefore, one can rewrite EQUATION (10) as the following.

$$\Psi(\theta, z, 0) = C_1 \left[C_3 \sin\left(\frac{Vz}{R_o}\right) + C_4 \cos\left(\frac{Vz}{R_o}\right) \right] e^{in_\theta \theta} \tag{11}$$

Second Boundary Condition

In the z-direction, the particle is in the $0 \leq z \leq L$. The particle is not allowed at $z = 0$ and $z = L$. Then, by this boundary condition, one can say that $\Psi(\theta, 0,0) = \Psi(\theta, L, 0)$. As a result, one can also reduce and define the value of $VL/R_o = n_Z \pi$. The n_Z is the z-quantum number and takes integer values ($n_z = 1, 2, 3, ...$).

$$\Psi(\theta, z, 0) = C_1 C_3 \sin\left(\frac{n_z \pi z}{L}\right) e^{in_\theta \theta} \tag{12}$$

Calculating the coefficient $C_1 C_3$

The wave function $\Psi(\theta, z, 0)$ should be normalized. The normalized wave function guarantees the existence of the particle in the system. Using the procedure for normalization, one can find that:

$$\int_0^{2\pi} \int_0^{L} |\Psi(\theta, z, 0)|^2 (R_o d\theta) dz = 1 \rightarrow 2\pi R_o (C_1 C_3)^2 \int_0^{L} \sin^2\left(\frac{n_z \pi z}{L}\right) dz = 1 \tag{13}$$

Using $\cos(2x) = 1 - 2\sin^2 x$, one can find this following result:

$$2\pi R_o (C_1 C_3)^2 \left[\frac{L}{2}\right] = 1 \rightarrow C_1 C_3 = \frac{1}{\sqrt{\pi R_o L}} \tag{14}$$

Plugging the coefficient $C_1 C_3$ from EQUATION (14) back into EQUATION (12), the complete solution of the wave function is in the following relation:

$$\Psi(\theta, z, 0) = \frac{1}{\sqrt{\pi R_o L}} \sin\left(\frac{n_z \pi z}{L}\right) e^{in_\theta \theta} \tag{15}$$

From EQUATION (15), one may construct the probability density of the particle as follows:

$$\rho(\theta, z, 0) = |\Psi(\theta, z, 0)|^2 = \frac{1}{\pi R_o L} \sin^2\left(\frac{n_z \pi z}{L}\right) \tag{16}$$

The probability density of the particle in EQUATION (16) is independent of the θ-direction. EQUATION (16) is also similar to the probability density of the one-dimensional infinite potential well [8], but with a different constant. However, one already knows that the QPCS is a two-dimensional system. By EQUATION (16), one can say that this θ-dimension is cloaked, analogous to the x^5 in KK theory. Therefore, this is the first indication that the QPCS is an analog model of the KK theory.

Energy Solution

By the solutions of U and V, one can write the energy solution E. The energy E depends on two quantum numbers and two geometric parameters of the system (L and R_o). The dependence of E on those two quantum numbers indicates the system is quantized.

$$U^2 + V^2 = \frac{2mER_o^2}{\hbar^2} \tag{17}$$

$$E = E_{n_z,n_\theta}(L, R_o) = \frac{n_z^2\pi^2\hbar^2}{2mL^2} + \frac{\hbar^2}{2m}\left[\frac{n_\theta}{R_o}\right]^2 \tag{18}$$

The energy in EQUATION (18) indicates a non-degenerate type of energy in general (for different L and different R_o). That means for two distinct quantum states, one can find a unique value of the particle's energy (one-to-one correspondence) [8]. However, if one sets the specific condition for R_o and L, such as $R_o = L/\pi$ and $L = \pi R_o$, the indication of the degenerate type of energy appears (see EQUATION (19) and EQUATION (20)).

$$E = E_{n_z,n_\theta}(L, L/\pi) = \frac{n_z^2\pi^2\hbar^2}{2mL^2} + \frac{\hbar^2}{2m}\left[\frac{n_\theta\pi}{L}\right]^2 = \frac{\pi^2\hbar^2}{2mL^2}\left(n_z^2 + n_\theta^2\right) \tag{19}$$

$$E = E_{n_z,n_\theta}(\pi/R_o, R_o) = \frac{n_z^2\pi^2\hbar^2}{2m(\pi R_o)^2} + \frac{\hbar^2}{2m}\left[\frac{n_\theta}{R_o}\right]^2 = \frac{\hbar^2}{2mR_o^2}\left(n_z^2 + n_\theta^2\right) \tag{20}$$

In EQUATION (18), the energy contribution from $\boldsymbol{\theta}$-dimension is familiar. The form of the energy is $\boldsymbol{E \sim (n_\theta^2/R_o^2)}$, and again, it is similar to the energy form due to the contribution of the $\boldsymbol{p^5}$ in KK theory [3, 5]. This characteristic refers to the second indication that the QPCS is analogous to the KK theory.

TIME INDEPENDENT PERTURBATION THEORY

Some quantum systems have a complicated form of a potential $\hat{V}$. This complicated form of $\hat{V}$ obscures the ability of someone who wants to figure out the wave function Ψ_n and energy E_n solutions. There is a method to approximate the wave function and energy solutions for any quantum system using the so-called perturbation theory [8]. The basic idea of the perturbation theory is simple. Perturbation theory tries to approximate the solution by adding corrections to the solution of the solvable, simpler system [8]. In mathematical formulation, let $\hat{H}^{(0)}$ be the Hamiltonian of the solvable simple system, the total Hamiltonian $\hat{H}$ be:

$$\hat{H} = \hat{H}^{(0)} + g\hat{H}^{(1)} + g^2\hat{H}^{(2)} + \cdots \tag{21}$$

Analogous to the total Hamiltonian in EQUATION (21), the wave function and the energy are in EQUATION (22) and EQUATION (23). The illustration of the perturbation method for solving the Schrödinger equation is in FIGURE 2.

$$\Psi_n = \Psi_n^{(0)} + g\Psi_n^{(1)} + g^2\Psi_n^{(2)} + \cdots \tag{22}$$

$$E_n = E_n^{(0)} + gE_n^{(1)} + g^2E_n^{(2)} + \cdots \tag{23}$$

Here, the g denotes a coupling constant, and the superscript index at H, Ψ_n, and E_n indicates the order of the perturbation.

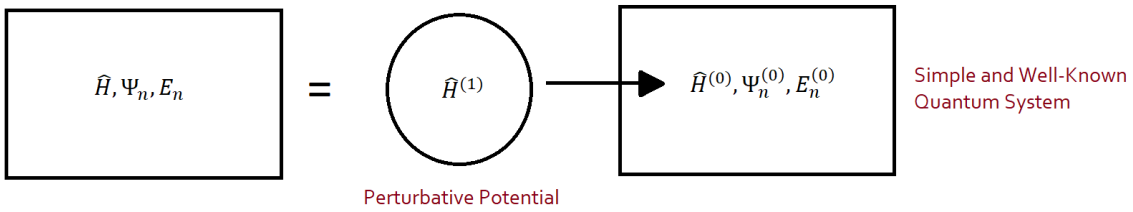

FIGURE 2. Illustration of the perturbation method for solving the Schrödinger equation

First-Order Perturbation

For the first-order perturbation, one can take the Hamiltonian in EQUATION (21), the wave function in EQUATION (22), and the energy in EQUATION (23) in the following form:

$$\hat{H} \approx \hat{H}^{(0)} + g\hat{H}^{(1)} \tag{24}$$

$$\Psi_n \approx \Psi_n^{(0)} + g\Psi_n^{(1)} \tag{25}$$

$$E_n \approx E_n^{(0)} + gE_n^{(1)} \tag{26}$$

EQUATION (24) to EQUATION (26) should be the solution of the Schrödinger equation. Therefore, by inserting EQUATION (24) to EQUATION (26) into the Schrödinger equation, one may obtain the following relation:

$$\hat{H}\Psi_n = E_n\Psi_n \rightarrow \hat{H}^{(0)}\Psi_n^{(1)} + \hat{H}^{(1)}\Psi_n^{(0)} = E_n^{(0)}\Psi_n^{(1)} + E_n^{(1)}\Psi_n^{(0)} \tag{27}$$

By taking the scalar product of EQUATION (27) with $\Psi_n^{(0)}$ and assuming $\Psi_n^{(0)}$ is an orthonormal wave function, one may obtain EQUATION (28):

$$\begin{aligned}\int_{V_i}\left[\Psi_m^{*(0)}\hat{H}^{(0)}\Psi_n^{(1)} + \Psi_m^{*(0)}\hat{H}^{(1)}\Psi_n^{(0)}\right] d^3\vec{r} \\ = \int_{V_i}\left[E_n^{(0)}\Psi_m^{*(0)}\Psi_n^{(1)} + E_n^{(1)}\Psi_m^{*(0)}\Psi_n^{(0)}\right] d^3\vec{r}\end{aligned} \tag{28}$$

If one takes $n = m$, EQUATION (28) reduces to EQUATION (29). EQUATION (29) is the so-called first-order energy correction.

$$\int_{V_i}\Psi_n^{*(0)}\hat{H}^{(1)}\Psi_n^{(0)} d^3\vec{r} = E_n^{(1)} \tag{29}$$

In the perturbation theory approach, the correction of the wave function should be composed of the well-known wave function (unperturbed wave function) by some linear combination constants, c_n, as represented in EQUATION (30).

$$\Psi_n^{(1)} = \sum_n c_n\Psi_n^{(0)} \tag{30}$$

To find c_n, one can use the orthonormality of the $\Psi_n^{(0)}$ with the following procedure:

$$\Psi_m^{*(0)}\Psi_n^{(1)} = \sum_n c_n \Psi_m^{*(0)}\Psi_n^{(0)} \rightarrow \int_{V_i} \Psi_m^{*(0)}\Psi_n^{(1)} d^3\vec{r} = \sum_n c_n \delta_{nm} = c_m \tag{31}$$

$$c_m = \int_{V_i} \Psi_m^{*(0)}\Psi_n^{(1)} d^3\vec{r} \tag{32}$$

Taking the result of EQUATION (28) and the hermicity of $\Psi_n^{(0)}$, one can obtain:

$$\left(E_n^{(0)} - E_m^{(0)}\right) \int_{V_i} \Psi_m^{*(0)}\Psi_n^{(1)} d^3\vec{r} = \int_{V_i} \Psi_m^{*(0)} \hat{H}^{(1)} \Psi_n^{(0)}\, d^3\vec{r} \tag{33}$$

$$c_m = \int_{V_i} \Psi_m^{*(0)}\Psi_n^{(1)} d^3\vec{r} = \frac{1}{E_n^{(0)} - E_m^{(0)}} \int_{V_i} \Psi_m^{*(0)} \hat{H}^{(1)} \Psi_n^{(0)}\, d^3\vec{r} \tag{34}$$

Therefore, one can obtain the complete expression of the $\Psi_n^{(1)}$ in the following form (one can replace n with m because n and m here are the dummy indices):

$$\Psi_n^{(1)} = \sum_m \left[\frac{1}{E_m^{(0)} - E_n^{(0)}} \int_{V_i} \Psi_n^{*(0)} \hat{H}^{(1)} \Psi_m^{(0)}\, d^3\vec{r}\right] \Psi_m^{(0)} \tag{35}$$

The above formulation from EQUATION (28) until EQUATION (35) assumes that the quantum system has a non-degenerate energy profile. For a degenerate energy profile, one can generalize $\Psi_n^{(0)}$ and $\Psi_n^{(1)}$ in the following form:

$$\Psi_n^{(0)} = c_\alpha \Psi_{n_\alpha}^{(0)} + c_\beta \Psi_{n_\beta}^{(0)} + c_\gamma \Psi_{n_\gamma}^{(0)} + \cdots \tag{36}$$

$$\Psi_n^{(1)} = c_\alpha \Psi_{n_\alpha}^{(1)} + c_\beta \Psi_{n_\beta}^{(1)} + c_\gamma \Psi_{n_\gamma}^{(1)} + \cdots \tag{37}$$

Here, α, β, γ, etc., label the different states with the same energy value. Then, the coefficients c ($c_\alpha, c_\beta, c_\gamma$, etc.) correspond to the linear combination coefficient of the mixture. By substituting EQUATION (36) and EQUATION (37) to EQUATION (27) and taking the scalar product with respective labels, one can build the matrix equation as the following:

$$\begin{bmatrix} H_{\alpha\alpha} & H_{\alpha\beta} & \cdots & H_{\alpha i} \\ H_{\beta\alpha} & H_{\beta\beta} & \cdots & H_{\beta i} \\ \vdots & \vdots & \ddots & \vdots \\ H_{i\alpha} & H_{i\beta} & \cdots & H_{ii} \end{bmatrix} \begin{bmatrix} c_\alpha \\ c_\beta \\ \vdots \\ c_i \end{bmatrix} = E_n^{(1)} \begin{bmatrix} c_\alpha \\ c_\beta \\ \vdots \\ c_i \end{bmatrix} \tag{38}$$

Solving the above matrix equation (secular equation), one can obtain the first-order energy correction and coefficient c ($c_\alpha, c_\beta, c_\gamma$, etc.) for degenerate cases.

STARK EFFECT IN QUANTUM MECHANICS

One of the successful pieces of evidence of quantum mechanics as a new theoretical framework in physics during the 19th - 20th century is the ability of quantum mechanics to predict the energy level of the hydrogen atom [8]. In addition, quantum mechanics also predicts the degeneracy among those energy levels theoretically [8]. The first evidence of this degeneracy among those energy levels is from the experiment of Johannes Stark in 1913 [6]. In this experiment, Stark used the electric field to see what happens with the energy levels of

the atom or molecule. The observation shows there is energy level-splitting [6, 8]. FIGURE 3 shows the Stark effect on the hydrogen and Rydberg atoms.

The energy level-splitting observed by Stark in 1913 is also well-described by the Schrödinger equation [9]. The mathematical model for the Stark effect is generally the formulation of the work needed to move a unit of electric charge (e.g., an electron, e) by the electric field. The EQUATION (40) shows the Stark effect Hamiltonian $\hat{H}_S$ (potential) in more detail.

$$\hat{H}_S = \int \vec{F}_E . d\vec{r} = \int \left(-e\vec{E}\right) . d\vec{r} = -e\vec{E} . \int d\vec{r} = -e\vec{E} . \vec{r} \tag{40}$$

Here, in the Stark effect Hamiltonian, the electric field $\vec{E}$ is independent of the particle's (charge) position $\vec{r}$ but may be time-dependent. Therefore, with the presence of the Stark Hamiltonian, the total Hamiltonian for the hydrogen atom can be written in EQUATION (41).

$$\hat{H} = \left[-\frac{\hbar^2}{2m}\nabla^2 - \frac{e^2}{4\pi\epsilon_o r}\right] + \left[-e\vec{E} . \vec{r}\right] \rightarrow \hat{H}\Psi = E\Psi \tag{41}$$

The EQUATION (41) can be solved by employing the perturbation theory in EQUATION (38), where the Stark Hamiltonian serves as the perturbative potential, and the system exhibits degeneracy.

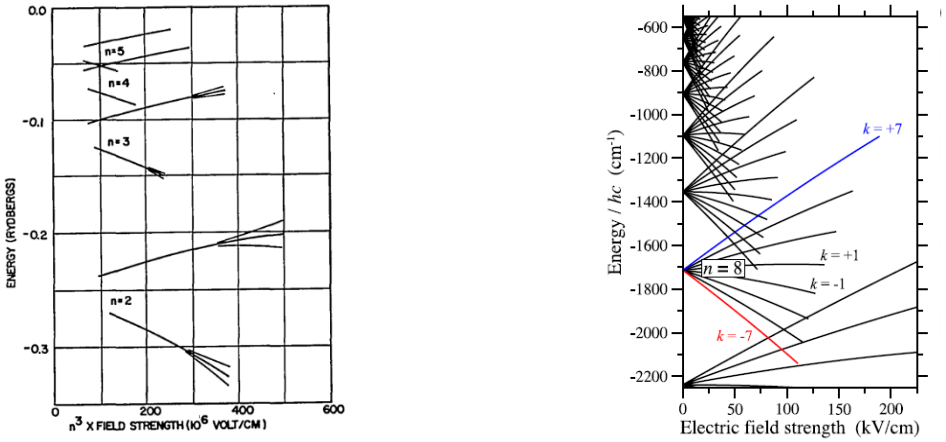

(a) (b)

FIGURE 3. The observation of Stark effect in (a) the hydrogen atom [10] and (b) in the Rydberg atom [11]. Here, the energy-splitting occurs and breaks the degeneracy.

RESULTS AND DISCUSSION

The main topic of this section is to see how the effect of Stark-like perturbative potential affects the energy of the QPCS up to the first-order correction. The first-order correction is considered in this calculation because it makes a significant contribution to the system behavior under perturbative potential. In addition, the perturbation method is used in this research because it relies on a small expansion parameter. The small expansion parameter leads to the convergence of the series expansion, which provides accurate results.

Stark-like Perturbative Potential and its effect on the QPCS

Stark-like perturbative potential ($\hat{H}_{SL}$) adapts the Stark perturbative potential ($\hat{H}_S$) in EQUATION (40). However, the electron charge e and the electric field $\vec{E}$ are replaced [12, 13, 14]. In this paper, they are changed into any arbitrary physical constant β and a vector function that depends on theta, $\vec{V}_o(\theta) = (V_{o_x}(\theta), V_{o_y}(\theta), V_{o_z}(\theta))$. Then, the $\hat{H}_{SL}$ for this research can be written in EQUATION (42):

$$\hat{H}_{SL} = \beta \vec{V}_o(\theta).\vec{r} \tag{42}$$

For the sake of simplicity to see the effect of the $\hat{H}_{SL}$ on the QPCS energy, the $\hat{H}_{SL}$ is projected along the z-axis of the system. Therefore, EQUATION (42) can be rewritten into EQUATION (43). In addition, for non-degenerate and degenerate cases, this research applies $\hat{H}_{SL}$ only to several low-excitation spectra only. This is discussed in more detail in the description below.

$$\hat{H}_{SL} = \beta V_{o_z}(\theta) z \tag{43}$$

Non-degenerate Case

The first-order correction of energy for the non-degenerate case $E_n^{(1)}$ is shown in EQUATION (29). By taking the unperturbed wave function $\Psi^{(0)}_{n_z,n_\theta}(\theta, z, 0)$ in EQUATION (15) and $\hat{H}_{SL}$ in EQUATION (43) to EQUATION (29), one can determine the $E^{(1)}_{n_z,n_\theta}$ as written in EQUATION (44).

$$E^{(1)}_{n_z,n_\theta} = \iint \Psi^{*(0)}_{n_z,n_\theta} \hat{H}_{SL} \Psi^{(0)}_{n_z,n_\theta} R_o \, d\theta dz = \frac{\beta}{\pi R_o L} \int_0^L z \sin^2\left(\frac{n_z \pi z}{L}\right) dz \int_0^{2\pi} V_{o_z}(\theta) d\theta \tag{44}$$

Using $\int_0^L z \sin^2\left(\frac{n_z \pi z}{L}\right) dz = \frac{1}{4}L^2$ for $n_z \in \mathbb{Z}$ and $n_z \geq 1$, then EQUATION (44) can be reduced into EQUATION (45) as in the following form.

$$E^{(1)}_{n_z,n_\theta} = \frac{\beta L}{4\pi R_o} \int_0^{2\pi} V_{o_z}(\theta) d\theta \tag{45}$$

From EQUATION (45), one can see that the first-order energy correction depends on the $V_{o_z}(\theta)$ only. This is the contribution from the Stark-like perturbative potential to the non-degenerate QPCS. In addition, there is no dependence on the QPCS quantum numbers n_z and n_θ for the non-degenerate case. This fact implies that the perturbation from the Stark-like perturbative potential to the QPCS has difficulty distinguishing between the effects in z-axis and the θ-direction. It can be seen easily by adding any functions of $V_{o_z}(\theta)$ to EQUATION (45), the result is a constant number. The energy level shift of each pair of QPCS quantum numbers is also constant. Thus, for the non-degenerate case, the Stark-like perturbative potential cannot be considered a means to reveal the extra dimension x^5, which is analogous to the cylindrical circumference in the QPCS.

Degenerate Case

As seen in the non-degenerate case, the Stark-like perturbative potential cannot uncloak the extra dimension (x^5) which is analogous to the cylinder circumference in the QPCS. In order to uncloak the extra dimension (x^5), let us jump to the degenerate case with the same Stark-like perturbative potential. The matrix element in EQUATION (38) can be determined as in EQUATION (47).

$$H_{ij} = \int_{V_i} \Psi_i^{*(0)}\, \hat{H}_{SL}\, \Psi_j^{(0)}\, d^3\vec{r} \tag{46}$$

$$H_{ij} = \beta R_o \int_0^{2\pi} \int_0^{L} \Psi_i^{*(0)} z V_{o_z}(\theta) \Psi_j^{(0)} d\theta dz \tag{47}$$

where $i, j = \{\alpha, \beta, \gamma, \dots\}$. In the QPCS case, there are two quantum numbers (n_z and n_θ). By choosing $R_o = L/\pi$ as mentioned in EQUATION (20), one can create the two-fold degenerate QPCS. Then, the index for i and j are only available for $i, j = \{\alpha, \beta\}$ and the perturbative matrix in EQUATION (38) only has a 2 × 2 matrix dimension.

In the degenerate QPCS, the wave function can be written as $\Psi_\alpha = \frac{1}{\sqrt{L^2}} \sin\left(\frac{n_{z_i}\pi z}{L}\right) e^{i n_{\theta_i}\theta}$ and $\Psi_\beta = \frac{1}{\sqrt{L^2}} \sin\left(\frac{n_{z_j}\pi z}{L}\right) e^{i n_{\theta_j}\theta}$. Here (n_{z_j}, n_{θ_j}) are the permutation of (n_{z_i}, n_{θ_i}) (e.g., $n_{z_i}, n_{\theta_i} = \{1,2\} \rightarrow n_{z_j}, n_{\theta_j} = \{2,1\}$). Substituting Ψ_α and Ψ_β to EQUATION (47), one can derive the matrix element in EQUATION (38) for the degenerate QPCS as follows:

$$H_{ij} = \frac{\beta R_o}{L^2} \int_0^{L} z \sin\left(\frac{n_{z_i}\pi z}{L}\right) \sin\left(\frac{n_{z_j}\pi z}{L}\right) dz \left[\int_0^{2\pi} V_{o_z}(\theta) e^{i\left(n_{\theta_j} - n_{\theta_i}\right)\theta} d\theta\right] \tag{48}$$

From the expression of the matrix element in EQUATION (48), one can see that the matrix element value for the degenerate QPCS depends on the quantum numbers.

To more clearly observe the effect of the Stark-like perturbative potential to the degenerate case of QPCS more clearly, this research takes the low-excitation energy level for simplicity. This means that this research considers only the following quantum number pairs:

$$(n_z, n_\theta) = \{(1,1), (1,2), (2,1), (2,2), (1,3), (3,1), (2,3), (3,2)\}$$

By substituting these set of quantum numbers into EQUATION (48), one can summarize the matrix elements for the low-excitation energy level of degenerate QPCS, as shown in TABLE 1 below.

TABLE 1. The Perturbation Matrix Element of the degenerate QPCS under the Stark-like Perturbative Potential. Here $I_o = \int_0^{2\pi} V_{o_z}(\theta)d\theta$, $I_1 = \int_0^{2\pi} V_{o_z}(\theta)e^{-i\theta}d\theta$, and $I_2 = \int_0^{2\pi} V_{o_z}(\theta)e^{i\theta}d\theta$

Quantum Number	Matrix Element H_{ij}
(1,1)	No Degeneracy
(1,2), (2,1)	$H_{\alpha\alpha} = H_{\beta\beta} = \frac{\beta L}{4\pi} I_o$ $H_{\alpha\beta} = -\frac{8\beta L}{9\pi^3} I_1 \; ; H_{\beta\alpha} = -\frac{8\beta L}{9\pi^3} I_2$
(2,2)	No Degeneracy
(1,3), (3,1)	$H_{\alpha\alpha} = H_{\beta\beta} = H_{\alpha\beta} = H_{\beta\alpha} = 0$
(2,3), (3,2)	$H_{\alpha\alpha} = H_{\beta\beta} = \frac{\beta L}{4\pi} I_o$ $H_{\alpha\beta} = -\frac{24\beta L}{25\pi^3} I_1 \; ; H_{\beta\alpha} = -\frac{24\beta L}{25\pi^3} I_2$

By employing the result in TABLE 1 and solving the secular equation in EQUATION (38), one can derive the first-order energy correction for the degenerate QPCS under the Stark-like perturbative potential as shown in EQUATION (51). TABLE 2 also summarizes the first-order energy correction for the degenerate QPCS under the Stark-like perturbative potential for (n_z, n_θ) from these following states: $\{(1,1),(1,2),(2,1),(2,2),(1,3),(3,1),(2,3),(3,2)\}$. FIGURE 4 illustrates the energy level splitting of the degenerate QPCS under the Stark-like perturbative potential.

$$\begin{bmatrix} H_{\alpha\alpha} & H_{\alpha\beta} \\ H_{\beta\alpha} & H_{\beta\beta} \end{bmatrix} \begin{bmatrix} c_\alpha \\ c_\beta \end{bmatrix} = E^{(1)} \begin{bmatrix} c_\alpha \\ c_\beta \end{bmatrix} \tag{49}$$

$$\begin{bmatrix} H_{\alpha\alpha} - E^{(1)} & H_{\alpha\beta} \\ H_{\beta\alpha} & H_{\beta\beta} - E^{(1)} \end{bmatrix} \begin{bmatrix} c_\alpha \\ c_\beta \end{bmatrix} = \begin{bmatrix} 0 \\ 0 \end{bmatrix} \tag{50}$$

$$E^{(1)}_{\alpha,\beta} = \frac{1}{2}\left(H_{\alpha\alpha} + H_{\beta\beta}\right) \pm \frac{1}{2}\sqrt{\left(H_{\alpha\alpha} + H_{\beta\beta}\right)^2 - 4\left(H_{\alpha\alpha}H_{\beta\beta} - H_{\beta\alpha}H_{\alpha\beta}\right)} \tag{51}$$

TABLE 2. First-order Energy Correction of the degenerate QPCS under the Stark-like perturbative potential

Quantum Number	First-order Energy Correction
(1,1)	No Degeneracy
(1,2), (2,1)	$E^{(1)}_{\alpha,\beta} = \frac{\beta L}{4\pi} I_o \pm \frac{8\beta L}{9\pi^3}\sqrt{I_1 I_2}$
(2,2)	No Degeneracy
(1,3), (3,1)	$E^{(1)}_{\alpha,\beta} = 0$
(2,3), (3,2)	$E^{(1)}_{\alpha,\beta} = \frac{\beta L}{4\pi} I_o \pm \frac{24\beta L}{25\pi^3}\sqrt{I_1 I_2}$

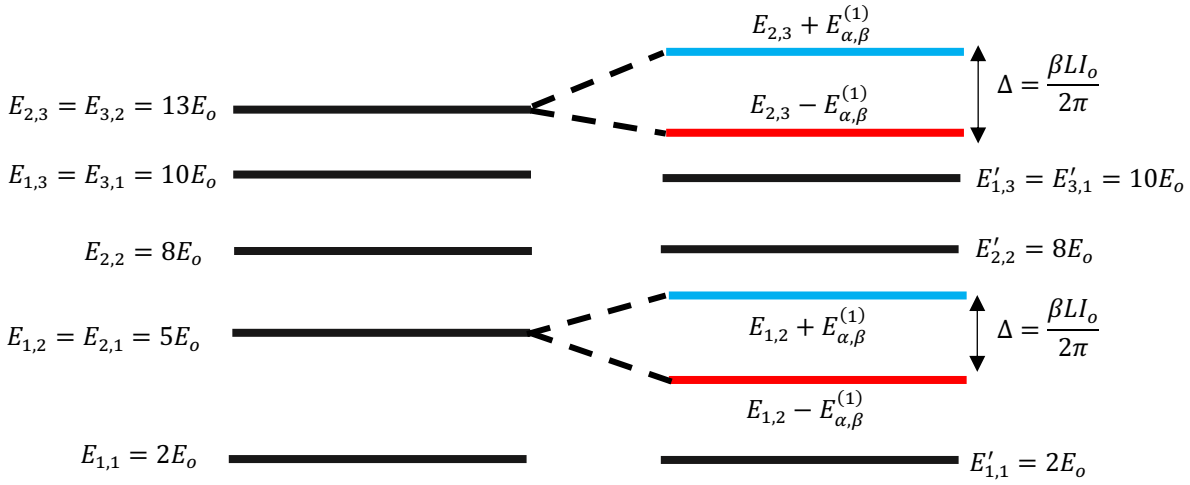

FIGURE 4. The illustration of the degenerate QPCS energy level shift due to the Stark-like Perturbative Potential.

From the result of TABLE 1, TABLE 2, and FIGURE 4, there is strong evidence that the degenerate QPCS under the Stark-like perturbative potential may open the opportunity to uncloak the extra dimension x^5 in KK theory (which is analogous to the θ variable in the QPCS). This is because the quantum numbers (n_z, n_θ) significantly determine the existence of the perturbation terms (as depicted by $H_{\alpha\beta}$ and $H_{\beta\alpha}$) which correspond to the splitting of the energy level. The energy-level splitting here is interpreted as the uncloaked extra dimension. The other factor that determines the existence of the perturbation terms is the expression of $V_{o_z}(\theta)$. If the strength of the $V_{o_z}(\theta)$ is large enough, the spliting in the energy levels also becomes larger. In addition, there are two remarks related to the application of the Stark-like perturbative potential to the QPCS.

Remark 1: Perturbative Splitting Rule

Let us return to the EQUATION (48). The first term of EQUATION (48) shows the integral:

$$\int_0^L z \sin\left(\frac{n_{z_i}\pi z}{L}\right) \sin\left(\frac{n_{z_j}\pi z}{L}\right) dz.$$

This integral depends purely on the position in z-axis and the quantum number in z-direction. This kind of integral is analogous to the dipole interaction with the dipole moment M [15, 16, 17, 18] as shown in EQUATION (52):

$$M \propto \int z\psi_i^*(z)\psi_j(z)\, dz \tag{52}$$

where the indices i and j correspond to quantum numbers of the state ψ. In the case of dipole moment, the selection rule of the dipole transition [17, 18] is particularly important to identify, and it can be obtained easily by checking which quantum numbers make EQUATION (52) non zero value ($M \neq 0$). In the Stark-like perturbative potential to the QPCS, the energi-level splitting exists if and only if the difference between n_{z_i} and n_{z_j} is ± 1. This leads to the so-

called "perturbative splitting rule" in the QPCS, and it should also be considered in the effort to uncloak the extra dimension.

$$\Delta n_z = \pm 1 \tag{53}$$

Remark 2: Strategy for choosing the $V_{o_z}(\theta)$

The existence of EQUATION (53) as the splitting rule requires anyone attempting to uncloak the extra dimension using the Stark-like perturbative potential to choose an appropriate $V_{o_z}(\theta)$ that satisfies EQUATION (54). EQUATION (54) ensures the splitting can be observed through experimental measurements.

$$\{I_1, I_2\} \in \mathbb{R} \quad \wedge \quad \{I_1, I_2\} \neq 0 \tag{54}$$

The only viable form of $V_{o_z}(\theta)$ that satisfies EQUATION (54) is a periodic potential in the θ-direction, as shown in EQUATION (55). Here, V_o and γ are nonzero constants, with $\gamma = \left\{\frac{1}{2}, \frac{3}{2}, \frac{5}{2}, \frac{7}{2}, \ldots\right\}$. This statement can be demonstrated by substituting a general polynomial function in θ-variable into I_1 and I_2.

$$V_{o_z}(\theta) = V_o \cos\theta \vee V_{o_z}(\theta) = V_o \sin\gamma\theta \tag{55}$$

Proof: Let us consider $V_{o_z}(\theta) = \sum_{k=0}^{\infty} a_k \theta^k$, then by the definition of I_1 and I_2, one can obtain the following results (EQUATION (56) and EQUATION (57)). The result shows that the integral values are complex numbers.

$$I_1 = \int_0^{2\pi} \left[\sum_{k=0}^{\infty} a_k \theta^k\right] e^{-i\theta} d\theta = \sum_{k=0}^{\infty} a_k \left[\int_0^{2\pi} \theta^k \cos\theta \; d\theta - i \int_0^{2\pi} \theta^k \sin\theta \, d\theta\right] \in \mathbb{C} \tag{56}$$

$$I_2 = \int_0^{2\pi} \left[\sum_{k=0}^{\infty} a_k \theta^k\right] e^{i\theta} d\theta = \sum_{k=0}^{\infty} a_k \left[\int_0^{2\pi} \theta^k \cos\theta \; d\theta + i \int_0^{2\pi} \theta^k \sin\theta \, d\theta\right] \in \mathbb{C} \tag{57}$$

Then, for the periodic potential $V_{o_z}(\theta) = V_o \cos\theta$,

$$I_1 = \int_0^{2\pi} [V_o \cos(\theta)] e^{-i\theta} d\theta = V_o \pi \in \mathbb{R} \tag{58}$$

$$I_2 = \int_0^{2\pi} [V_o \cos(\theta)] e^{i\theta} d\theta = V_o \pi \in \mathbb{R} \tag{59}$$

and for $V_{o_z}(\theta) = V_o \sin\gamma\theta$:

$$I_1 = \int_0^{2\pi} [V_o \sin(\gamma\theta)] e^{-i\theta} d\theta = \frac{2V_o \sin(\gamma\pi)}{\gamma^2 - 1} (\gamma \sin(\gamma\pi) - i \cos(\gamma\pi)) \in \mathbb{R}, \quad \text{if } \gamma \in \left\{\frac{1}{2}, \frac{3}{2}, \frac{5}{2}, \ldots\right\} \tag{60}$$

$$I_2 = \int_0^{2\pi} [V_o \sin(\gamma\theta)] e^{i\theta} d\theta = \frac{2V_o \sin(\gamma\pi)}{\gamma^2 - 1} (\gamma \sin(\gamma\pi) + i \cos(\gamma\pi)) \in \mathbb{R}, \quad \text{if } \gamma \in \left\{\frac{1}{2}, \frac{3}{2}, \frac{5}{2}, \ldots\right\} \tag{61}$$

These kinds of periodic potentials in EQUATION (55) as an implication of the perturbative splitting rule, may also provide an alternative insight regarding the physics that uses the extra

dimension (e.g., KK theory). These areas of physics include the UV completion in multi-natural inflation model and SUSY-breaking model [19], and the implementation of optical lattice technology to simulate D+1-dimensional quantum system using D-dimensional platforms [20]. In addition, studying the possibility of uncloaking an extra dimension using a QPCS can have several experimental implications. The experimental setups could be designed to test these predictions. The following are examples of experimental setups that could potentially validate the theoretical results:

1. Quantum particles like electrons confined in cylindrical nanostructures like carbon nanotubes (CNT) or semiconductor nanowires could serve as physical realizations of your QPCS model. If an extra spatial dimension influences the energy spectrum, specific shifts in energy levels could be detected via tunneling spectroscopy or photoluminescence measurements [21, 22].
2. Ultra-cold atoms trapped in a toroidal optical potential may simulate the quantum confinement effects in cylindrical geometry. By introducing an artificial gauge field (analogous to the Stark-like perturbation), one could study whether the energy spectrum exhibits signatures of an extra dimension [23, 24].
3. Semiconductor quantum rings allow for electron confinement along curved geometries [25]. Applying external fields (electric/magnetic) could mimic the Stark-like perturbative potential in theory. If the observed energy level splitting patterns match theoretical predictions, it could suggest an underlying extra-dimensional effect.
4. Graphene nanoribbons or curved 2D materials could serve as a condensed matter analogs to test cylindrical confinement effects [26]. If an extra dimension alters the electronic band structure, it might be observable through transport or optical experiments.
5. In amorphous materials, atoms are not arranged in a periodic lattice but rather in a disordered structure. Despite this, local atomic arrangements still obey geometric constraints, which are reflected in the radial distribution function (RDF), $G(r)$—a function that describes how atomic density varies as a function of distance [27, 28]. If an extra dimension subtly influences interatomic interactions, this effect could leave an imprint on the RDF, such as:
   i. unusual decay rates in $G(r)$, particularly in the long-range correlations,
   ii. anomalous broadening or shifting of peaks in $G(r)$, suggesting modifications to interatomic forces, and
   iii. new oscillatory features not predicted by conventional three-dimensional amorphous structure models.

   This because the RDF is fundamentally tied to the underlying dimensionality of space. To test whether extra-dimensional effects modify $G(r)$ in amorphous materials, the following experimental techniques could be applied:

   i. **Neutron and X-ray Scattering**, which measure structure factors $S(q)$, which are related to $G(r)$ through a Fourier transform or Wavelet Transform [27, 28].

Unexpected deviations in $S(q)$ at certain length scales could indicate hidden dimensional influences, and

ii. **Temperature-Dependent Studies**, where if extra dimensions modify atomic interactions, thermal expansion or disordering effects might show unconventional trends compared to standard 3D models.

CONCLUSION

The Kaluza-Klein (KK) theory is one of the theoretical frameworks that aims to unify gravitational and electromagnetic interactions by introducing an additional spatial dimension, denoted as x^5. In this theory, the extra dimension is compactified to a small size, effectively concealing its presence. This compactification provides a compelling explanation for why gravity is significantly weaker than electromagnetism at observable scales. This study investigates a possible method to reveal the hidden extra dimension in KK theory by applying a Stark-like perturbative potential, represented as $\widehat{H}_{SL} = \beta z V_{o_z}(\theta)$, to a non-relativistic quantum particle confined to a cylindrical surface (QPCS) with radius R_o and length L. The QPCS system is chosen because its angular coordinate θ plays a role analogous to the extra dimension in KK theory. In the non-degenerate case, the Stark-like perturbative potential shifts the energy levels of the QPCS but does not distinguish the extra dimension. However, in the degenerate case $(R_o = L/\pi)$, the perturbation induces energy level splitting, making the contribution from the angular coordinate θ identifiable. These findings suggest a potential approach to detecting extra-dimensional effects in KK theory, which could be tested experimentally using carbon nanotubes (CNTs), semiconductor nanowires, trapped ultra-cold atoms, semiconductor quantum rings, graphene nanoribbons, and amorphous materials. For future research, a comparative analysis of the stark-like perturbative potential with other perturbative effects, such as Zeeman-like, anharmonic-like, or additional well-known perturbative schemes, could help identify the most effective method for unveiling the presence of extra dimensions.

REFERENCES

[1] T. Kaluza, "Zum Unitätsproblem in der Physik," *Sitzungsber. Preuss. Akad. Wiss. Phys. Math. Klasse*, vol. 966, pp. 966–972, 1921. [Online]. Available: https://inspirehep.net/literature/14621

[2] O. Klein, "Quantentheorie und fünfdimensionale Relativitätstheorie," *Z. Phys.*, vol. 37, pp. 895–906, 1926. doi: 10.1007/BF01397481.

[3] T. Applequist, A. Chodos, and P. G. O. Freund, *Modern Kaluza-Klein Theories*. Reading, MA: Addison-Wesley, 1987.

[4] B. Zwiebach, *A First Course in String Theory*. Cambridge: Cambridge University Press, 2004.

[5] N. Deutschmann, "Compact Extra Dimensions in Quantum Mechanics," *arXiv:1611.01026* [physics.gen-ph], 2017. doi: 10.48550/arXiv.1611.01026.

[6] J. Stark, "Observations of a separation of spectral lines by an electric field," *Nature*, vol. 92, p. 401, 1913. doi: 10.1038/092401b0.

[7] K. Hentschel, "Stark Effect," in *Compendium of Quantum Physics*, D. Greenberger, K. Hentschel, and F. Weinert, Eds. Berlin, Heidelberg: Springer, 2009, pp. 738–742.

[8] D. J. Griffiths and D. F. Schroeter, *Introduction to Quantum Mechanics*, 3rd ed. Cambridge: Cambridge University Press, 2018.
[9] P. S. Eipstein, "The Stark Effect from the point of view of Schroedinger's Quantum Theory," *Phys. Rev.*, vol. 28, pp. 695–701, 1926. doi: 10.1103/PhysRev.28.695.
[10] M. H. Rice and R. H. Good, "Stark Effect in Hydrogen," *J. Opt. Soc. Am.*, vol. 52, pp. 239–246, 1962.
[11] S. D. Hogan, "Rydberg-Stark deceleration of atoms and molecules," *EPJ Tech. Instrum.*, vol. 3, no. 2, 2016. doi: 10.1140/epjti/s40485-015-0028-4.
[12] M. Ben-Artzi, "An Application of Asymptotic Techniques to certain problems of Spectral and Scattering Theory of Stark-like Hamiltonians," *Trans. Amer. Math. Soc.*, vol. 278, pp. 817–839, 1983. doi: 10.1090/S0002-9947-1983-0701525-6.
[13] M. Ben-Artzi, "Unitary Equivalence and Scattering Theory for Stark-like Hamiltonians," *J. Math. Phys.*, vol. 25, no. 4, pp. 951–964, 1984. doi: 10.1063/1.526212.
[14] J. F. Bony et al., "Scattering Theory for the Schrödinger equation with repulsive potential," *J. Math. Pures Appl.*, vol. 84, pp. 509–579, 2005. doi: 10.1016/j.matpur.2004.10.007.
[15] P. H. Krupenie and W. Benesch, "Electronic transition moment integrals for first ionization of CO and the A-X transition in CO+. Some limitations on the use of the r-centroid approximation," *J. Res. Natl. Bur. Stand. A Phys. Chem.*, vol. 72A, no. 5, pp. 495–503, 1968. doi: 10.6028/jres.072A.042
[16] B. Simmen, E. Mátyus, and M. Reiher, "Electric transition dipole moment in pre-Born-Oppenheimer molecular structure theory," *J. Chem. Phys.*, vol. 141, no. 15, 2014. doi: 10.1063/1.4897632.
[17] P. C. Desmukh, *Quantum Mechanics – Formalism, Methodologies, and Applications*. Cambridge: Cambridge University Press, 2024.
[18] D. H. McIntyre, *Quantum Mechanics: A Paradigms Approach*. Boston, MA: Pearson Education Inc., 2012.
[19] T. Higaki and Y. Tatsuta, "Inflation from periodic extra dimensions," *JCAP*, vol. 07, p. 011, 2017. doi: 10.1088/1475-7516/2017/07/011.
[20] O. Boada et al., "Quantum simulation of an extra dimension," *Phys. Rev. Lett.*, vol. 108, 2012. doi: 10.1103/PhysRevLett.108.133001
[21] A. Baltenkov and A. Msezane, "Electronic quantum confinement in cylindrical potential well," *Eur. Phys. J. D*, vol. 70, p. 81, 2016. doi: 10.1140/epjd/e2016-60728-2
[22] E. G. Barbagiovanni et al., "Quantum confinement in Si and Ge nanostructures: Theory and experiment," *Appl. Phys. Rev.*, vol. 1, p. 011302, 2014. doi: 10.1063/1.4835095
[23] A. Chakraborty et al., "A toroidal trap for cold 87Rb atoms using an rf-dressed quadrupole trap," *J. Phys. B: At. Mol. Opt. Phys.*, vol. 49, p. 075304, 2016. doi: 10.1088/0953-4075/49/7/075304
[24] S. K. Schnelle et al., "Versatile two-dimensional potentials for ultra-cold atoms," *Opt. Express*, vol. 16, pp. 1405–1412, 2008. doi: 10.1364/OE.16.001405
[25] J. Kim, L. W. Wang, and A. Zunger, "Prediction of charge separation in GaAs/AlAs cylindrical nanostructures," *Phys. Rev. B*, vol. 56, p. R15541, 1997. doi: 10.1103/PhysRevB.56.R15541
[26] M. Hbibi et al., "Finite confinement potentials, core and shell size effects on excitonic and electron-atom properties in cylindrical core/shell/shell quantum dots," *Sci. Rep.*, vol. 12, p. 14854, 2022. doi: 10.1038/s41598-022-19118-3
[27] D. Senjaya, A. Supardi, and A. Zaidan, "Theoretical formulation of amorphous radial distribution function based on wavelet transformation," *AIP Conf. Proc.*, vol. 2314, no. 1, p. 020001, 2020. doi: 10.1063/5.0034410

[28] D. Senjaya and A. Zaidan, “Wavelet transform amorphous radial distribution function validation using classical density functional theory with Born-Meyer type potential,” *AIP Conf. Proc.*, vol. 2554, no. 1, p. 050002, 2023. doi: 10.1063/5.0103690